Multiple magnetic-phase transitions and critical behaviour of charge-density wave compound $TbTe_3$

Z. Yang,[1] A. J. Drew,[1] S. van Smaalen,[2] N. van Well,[2] F. L. Pratt,[3] G. B. G. Stenning,[3] A. Karim,[4] and K. Rabia[5,*]

[1]*School of Physics and Astronomy, Queen Mary University of London, 327 Mile End Road, London E1 4NS, UK*
[2]*Laboratory of Crystallography, University of Bayreuth, 95440 Bayreuth, Germany*
[3]*ISIS Facility, STFC Rutherford Appleton Laboratory, Harwell Oxford, Oxfordshire OX11 0QX, UK*
[4]*Applied Physics computer and Instrumentation Center, PCSIR Labs. complex,Karachi 75280, Pakistan*
[5]*Physics Department, COMSATS University Islamabad, Park Road, Tarlai Kalan, Islamabad 45550, Pakistan*

(Dated: December 8, 2019)

We report the multiple magnetic phase transitions and critical behaviour of 2D charge-density wave (CDW) compound $TbTe_3$ studied by μSR measurements and dc magnetization measurements. Zero-field μSR has shown three magnetic transitions below 7 K. The longitudinal field measurements under 50 G has confirmed the first transition at T_N = 6.3 K. Scaling analysis from above T_N gives the critical exponent w = 0.63(5), suggesting the Ising 3D antiferromagnetic nature of the ordering, which is likely mediated by the 2D correlations. However, the obtained w = 0.81(5) below T_N indicates the ferromagnetic phase, which arises over the multiphase transitions at lower temperatures. Temperature-dependent transverse frequency shift gives a relatively smaller exponent γ = 1.0(1) than the Ising 3D model. The different transitions were also observed by dc magnetization measurements, suggesting two magnetic transitions at 7.4 K and 3.1 K, which correspond to the antiferromagnetic and ferromagnetic phases respectively.

I. INTRODUCTION

Low-dimensional materials with highly anisotropic electronic structure often exhibit electronic instabilities that can lead to superconductivity or charge-density-wave phenomena. Charge-density-waves (CDWs) in low-dimensional materials are predominantly driven by Fermi-surface nesting.[1] The formation of CDW is expected to affect the magnetic properties of the material because of the change in the density of states at Fermi level.[2] The quasi-2D rare-earth tritelluride ($RETe_3$) compounds with RE = Y, La-Sm, Gd-Tm, crystallizes in an orthorhombic structure with space group Cmcm.[3] The double layer of square Te-sheets form two-dimensional (2D) electronic bands and the RETe-slabs between two square Te-sheets contribute to magnetism[4–6] The lattice parameters a and c are close to each other and have a value of $\approx$ 4.5 Å, whilst b $\approx$25 Å is 5.5 times larger than a and c. Therefore, there is a large anisotropy between ac plane and b axis.[3]

The unique feature of $RETe_3$ compounds is the multiple CDW transitions at different temperatures[7–12] with the coexistence of long-range magnetic order (LRMO) below 10K.[13–15] $TbTe_3$ is the most studied compound from the family of $RETe_3$. It has a CDW as a stable ground state at room temperature and undergoes two more CDW phase transitions observed at 41 K[3] and 5 K.[7] Notably, in $TbTe_3$, a third CDW phase coexists with the magnetic order at $\sim$5 K. Ru *et al*.[2] firstly revealed the multiple magnetic phase transitions in $TbTe_3$ by magnetization, heat-capacity, and electrical resistivity measurements. Three closely-spaced magnetic phase transitions were suggested at 5.5($\pm$0.25) K, 5.79($\pm$0.25) K, and at 6.0($\pm$0.25) K. The temperature value in parenthesis is the approximate difference of the transition temperature measured for data with different techniques. By neutron diffraction, Pfuner *et al*.[16] confirmed two of the three magnetic phase transitions at about 5.8 K on the higher temperature side and at about 5.3 K on the lower side. The magnetic order was suggested to be incommensurate at 5.8 K, which turns into commensurate below 5.3 K. Pfuner *et al*. also suggested that the magnetic Bragg peak position (0, 0, 0.24) is close to the propagation vector associated with the lattice modulation at high temperature, which is incommensurate in the CDW state at down to 5 K according to Ref.[17]. It has raised the possibility that the LRMO is linked to the modulated structure in the CDW state, although further work is needed to investigate how the CDW and magnetic order may interact with each other. In a more recent work by Saint-Paul *et al*.[13], through sound velocity and ultrasonic attenuation measurements, three successive transitions were suggested at $T_{mag1} \sim$ 6.5 K, $T_{mag2} \sim$ 5.8 K, and $T_{mag3} \sim$ 5.3 K. Despite that the lower two temperatures agree with Ref.[2] and Ref.[16], Saint-Paul *et al*. indicated that the first transition should occur at a higher temperature at around 6.5 K rather than 5.8 K.

Despite the mentioned studies in the complex characteristics of the multiple CDW states, the magnetic structures of $TbTe_3$ and the critical phenomena regarding the magnetic transitions are poorly explored. Here we report the first study of the critical behavior associated with the magnetic transitions in $TbTe_3$ by combining muon spin rotation/relaxation (μSR) and magnetometry measurements. μSR is an ideal choice for probing local dynamics, especially for studying the static and dynamic magnetic properties in various systems[18–20]. It provides an approach to the interactions between magnetic order, fluctuations and superconductivity[21]. μSR has been proved successful in studying the critical behaviors by combined three different types of measurements: in zero-field (ZF), longitudinal field (LF), and under transverse field (TF)[22–24]. We will identify the multiple magnetic transitions from ZF-μSR and magnetometry, and make critical analysis via both LF relaxation and TF frequency shift.

II. EXPERIMENTAL DETAIL

Single crystals of $TbTe_3$ were grown by the self-flux method at the Laboratory of crystallography, University of Bayreuth, Germany, according to the procedures described by Ru and Fisher[6,25]. About 100 mg of unoriented mosaic crystals were

placed onto a 1×1 cm^2 silver plate with vacuum grease. A fly-past holder was used, with four silver 25 μm sheets placed in front. The sample was then wrapped in a 5 μm aluminium packet for the μSR experiments.

The μSR measurements were performed on the high magnetic field (HiFi) spectrometer at the ISIS muon facility, Rutherford Appleton Laboratory (RAL) in UK. The measurements were carried out in the low temperature range 2-10 K using a helium cryostat, in zero, longitudinal and transverse applied magnetic field. During the μSR experiment, the muons were implanted into the sample, with their spin polarised antiparallel to the momentum. The muon then stopped and sit within the sample, before it decayed into a positron and neutrinos, with a lifetime of 2.2 μs. The muon spin asymmetry A(t), which is related to the spin polarisation, was measured as a function of time.[26]

The magnetometry measurements were performed using a commercial (Quantum Design MPMS) SQUID magnetometer covering the temperature range 2-300 K, under magnetic field of 50 Oe and 1000 Oe.

III. RESULTS AND DISCUSSION

A. ZF-μSR

The ZF-μSR spectra measured on $TbTe_3$ at different temperatures are shown in Fig. 1 (a). The data were fitted to a combined function of Lorentzian exponential and static Gaussian relaxation;

$$A(t) = A_{Lor}\exp(-\lambda t) + A_{Gau}\exp(-\Delta^2 t^2/2) + A_{BG}. \quad (1)$$

It is found that the Gaussian component is temperature independent and contributes to asymmetry of about $A_{Gau} = 5.5\%$, with the rms field width of $\Delta = \gamma_\mu B_{local} = 0.25$ MHz on average, where $\gamma_\mu = 2\pi\times135.5$ MHz T^{-1} is the muon gyromagnetic ratio. This suggests that the Gaussian component comes from the muon seeing random static moments from the sample holder or in the cryostat. Thus, we have re-fitted the data, with the Gaussian term fixed as a background. The Lorentzian asymmetry, resulting from the dynamic electron spins, has seen a dramatic decrease on cooling from about 7.5 to 6 K, suggesting the slowing down of the Tb spin fluctuation and the forming of LRMO (Fig. 1 (a)).

In Fig.1 (b) and (c), the vertical dashed lines represent the three transitions at $T_{mag1} \sim 6.5$ K, $T_{mag2} \sim 5.8$ K and $T_{mag3} \sim 5.3$ K according to Ref.[13,16] The ZF relaxation rate exhibits a broad peak around the three transitions, with some up-and-downs that agree quite well with the mentioned transition temperatures. Furthermore, the shaded gray region in the inset of Fig.1(a), promising 2D correlations are likely in play according to Ref.[16] There seems a slight increase of asymmetry below 5 K, although the relaxation rate tends to flatten.

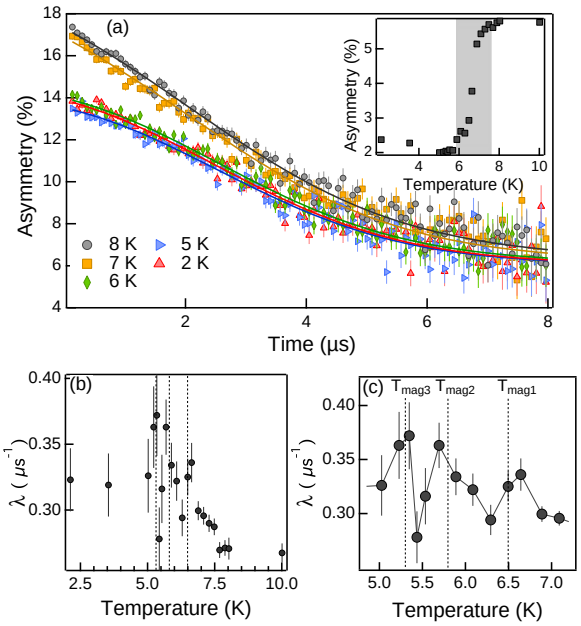

FIG. 1. (Color online) The results from ZF-μSR on $TbTe_3$ as a function of temperature. (a) The asymmetry spectra were fitted with a function of two components: Lorentzian and Gaussian (fixed). The inset plot shows the asymmetries of the Lorentzian component, which dropped dramatically from about 7.5 to 6 K (the gray area). (b) The relaxation rate of the Lorentzian component. The vertical dashed lines denote the three magnetic transition temperatures, which can be seen more clearly in (c). (c) The zoomed in of plot-(b) for 5-7 K, the three transition were suggested at T_{mag1} ~6.5 K, T_{mag2} ~5.8 K, and T_{mag3} ~5.3 K,[2,13,16] the dashed lines are guide for the eyes.

B. LF-μSR

We have applied various longitudinal fields in the range 0.1-5000 G along the incident muon spin, just below the magnetic phase transitions at 5 K, and at 2 K. The applied longitudinal field tends to decouple the muon spin from the local field at 50 G, and restores the muon spin polarisation. The LF time spectra in a range 0.1-30 G are fitted by using (1), above 30 G, the Gaussian shape started to suppressed and completely disappear at 50 G. The selected time spectra along with the fit at 5 K are shown in Fig. 2 (a). The integrated asymmetry is plotted in Fig. 2 (b) as a function of the applied field. The arrow denotes where the muon spin is decoupled from the local field at 50 G, which is sensed indirectly by the muon.

In order to better study the temperature dependent fluctuations of the Tb^{3+} spin, we have applied the magnetic field of 50 G, which suppressed the Gaussian background as discussed. The temperature dependent measurements were carried out across the magnetic phase transition region from 8 to 2 K. The μSR time spectra under LF of 50 G at different temperatures are sown in Fig. 3 (a). It is very clear that the applied field has suppressed the Gaussian component visible in the ZF, enabling one to achieve a better fit for the critical dynamic fluctuations of the electronic spin. The asymmetry data are fitted to the function of exponential decay A(t)= $A_0\exp(-\lambda t)$. The spin

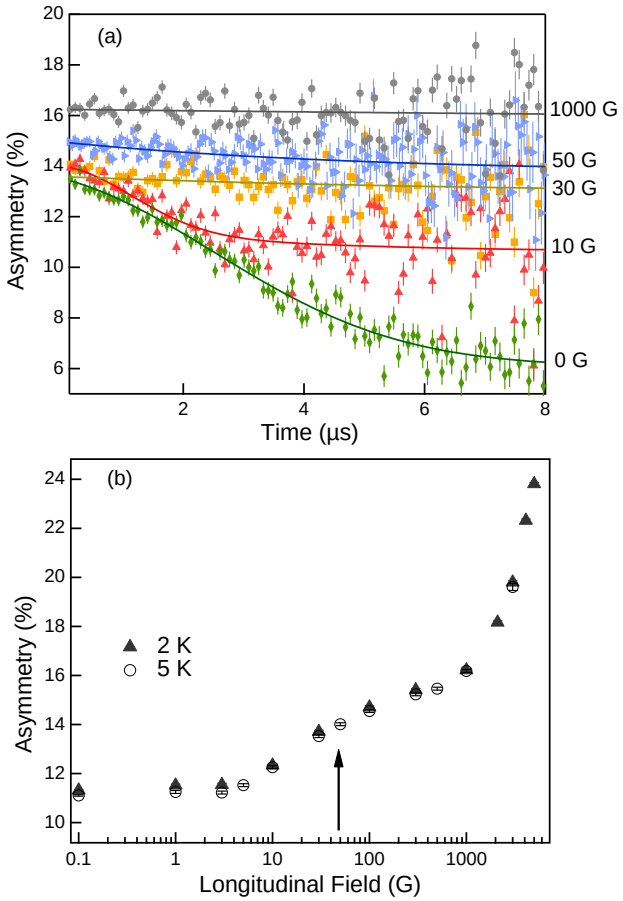

FIG. 2. (Color online) (a) The asymmetry spectra at 5 K. As the applied longitudinal field increases, the Gaussian shape becomes completely suppressed at 50 G and above, where the coupling of muon spin with the local field is suppressed. (b) The integrated asymmetry vs the applied longitudinal field, the arrow denotes the decoupling field≈ 50 G.

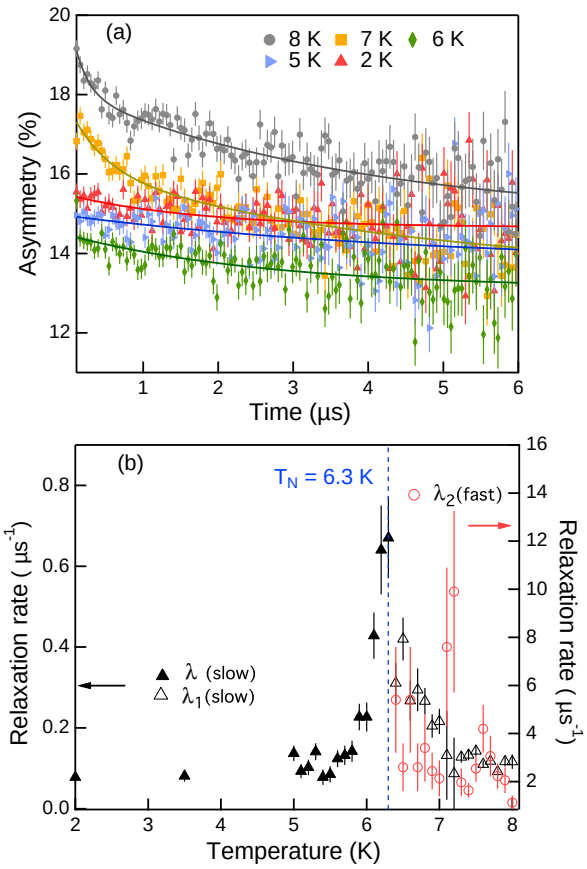

FIG. 3. (Color online) (a) The LF-μSR asymmetry under 50 G at various temperatures, along with the fit (solid lines) as described in the main text. (b) The temperature dependence of relaxation rates extracted from the fits. The blue dashed line denote the transition at6.3K

lattice relaxation rates obtained from the fitting is shown in Fig. 3 (b). One magnetic transition is clearly seen at T_N = 6.3 K, such a transition temperature is indeed very close to T_{mag1} suggested by Ref.[13], which was evidenced in our ZF results.

We did not see obvious evidence for T_{mag2} and T_{mag3} here. This is probably due to the fact that, under the external field, the additional transitions at lower temperatures cannot be resolved anymore using a single relaxing function. It is, however, easier for us to model the critical phenomenon approaching T_N from both sides. Below T_N the muon asymmetry can be fitted by a single exponential function, which gives λ (slow) as the Tb spin becomes static. Above the transition, a second term with the fast relaxation rate λ_2 is needed, which takes account for the early time fast relaxation that arises. λ_2 is ∼20 times bigger than the slow component. But below T_N, this fast component goes beyond the upper frequency limit of ISIS. Nevertheless, λ_1 (slow) has the same scale as λ, and decreases as the temperature goes up, when the thermal fluctuations increases.

The T_N of 6.3 K confirmed by the LF measurements is close to T_{mag1}, and the temperature dependence of the relaxation rate allows us to study the critical region around T_N. Using scaling analysis separately for λ and λ_1, we studied the critical fluctuations below and above T_N, respectively. The muon longitudinal relaxation rate, in the fast fluctuation limit, is directly proportional to the spin-spin correlation time[22]: $\lambda \sim \tau \sim |1 - T/T_N|^{-w}$. The fit for the two relaxation rates gives the critical exponent $w = 0.81(5)$ and $w = 0.63(5)$ for λ and λ_1, respectively (see Fig. 4). The w is higher for $T < T_N$ than that above T_N, which is likely because of the additional transitions are present in a range of 6-5 k, at around T_{mag2} and T_{mag3}. The expected critical exponents for different magnetic models are listed in table I and discussed in Section E.

C. TF-μSR

We have also performed μSR measurements in a transverse magnetic field of 50 G, to study the critical phenomenon approaching T_N associated the critical exponent γ. The oscillatory polarization spectra at 7 K and at 6.3 K, well above and just

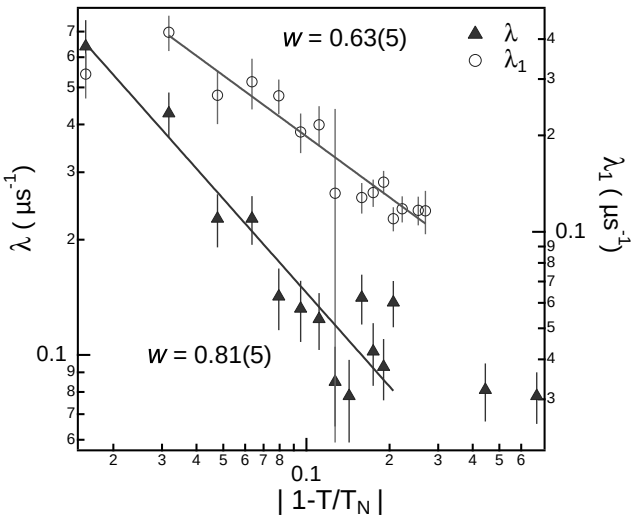

FIG. 4. (Color online) The critical scaling analysis for LF muon spin relaxation rates above and below T_N = 6.3 K. The solid lines are the fits according to $\lambda \propto |1 - T/T_N|^{-w}$.

upon the transition, respectively, are shown in Fig. 5 (a). It can be seen that the TF data reveal a modest drop in initial asymmetry on cooling from 7K to 6.3K, this means the fraction of muons were either in large internal field (probably from the electron spin), which is too high to resolve or relaxes within ten of nanosecond. The rest were subjected to a narrower (or faster fluctuating) field distribution at 6.3K. In our present modeling one single relaxing oscillation term is simply used. It may well be that the signal from the background (silver and grease, etc.) is contained in the exponentially relaxing term. Nevertheless, one would not expect the oscillating frequency to be affected too much by the background, as the oscillation is such obvious and dominating and our focus is on the frequency shift. The spectra are fitted by the oscillation exponential decay function given below;

$$A(t) = A_0 \cos(ft + \phi) \exp(-\lambda t) \qquad (2)$$

where A_0 is the initial asymmetry, f is the frequency of the muon spin oscillation and ϕ is the phase constant. The precession frequency f provides a way of obtaining the frequency shift, with regards to the internal local field, when approaching the phase transition.

The frequency shift due to magnetic fluctuations can be modelled by[22] $(f/f_0 - 1) \propto \chi \propto (T/T_N - 1)^{-\gamma}$. The critical scaling is plotted in Fig.5 (b), which gives the exponent $\gamma = 1.0(1)$. In Fig.5 (b) close to T_N the two points are not reliable due to the influence of background signal and avoided in fit. The comparison of critical exponent in detail is given in discussion part.

D. MAGNETOMETRY RESULTS

The temperature-dependent of dc-magnetization measurements on $TbTe_3$ single crystal were performed by zero-field

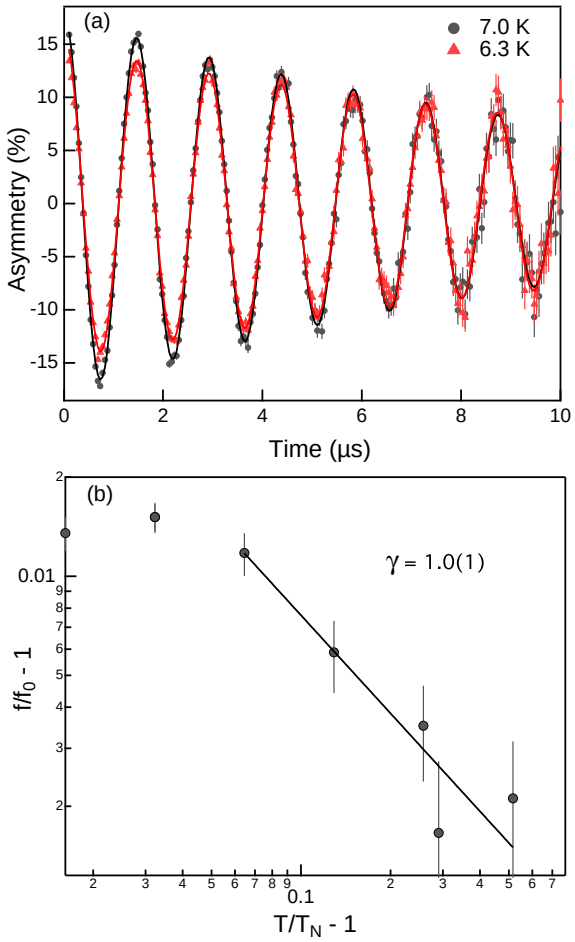

FIG. 5. (Color online) (a) The μSR asymmetry spectra measured at 7 K and 6.3 K under transverse field of 50 G. The asymmetry is reduced when approaching T_N, as a result of suppressed fluctuations. The data is fitted by using the oscillatory exponential decay function. (b) The critical scaling analysis for TF frequency shift above T_N, which is fitted by $(f/f_0 - 1) \propto (T/T_N - 1)^{-\gamma}$.

cooling (ZFC) and field cooling (FC) in random orientation with the applied field of 50 Oe and 1000 Oe. The data collected in a temperature range 300-2 K is shown in Fig. 6(a) and (b). The two field measurements present consistent behaviour, which agrees with the LF-μSR results in Fig.2 that one needs a field higher than 1000 Oe to significantly align the moments. The zoomed images of magnetization, shown in the insets of Fig. 6 (a) and (b) show two magnetic phase transitions below 10 K. The two transitions can be more clearly seen from the inverse susceptibility ($\chi^{-1} = H/M$) plots in Fig. 6 (c) to occur at 7.4 K and 3.1 K.

The Curie constant C = 4.7874(4) emu mol^{-1} K from the 50 Oe fit and C=7.3304(5)emu mol^{-1} K from the 1000 Oe result. We have made a Curie-Weiss fit according to $\chi^{-1} \propto (T - \theta)/C$ for the paramagnetic regime 20-300 K. The fit gives the Curie-Weiss temperature of θ = -19.27(2) K from the 50 Oe data, and θ = -17.47(1) from the 1000 Oe data. The negative sign strongly supports the AFM feature of the first transition at

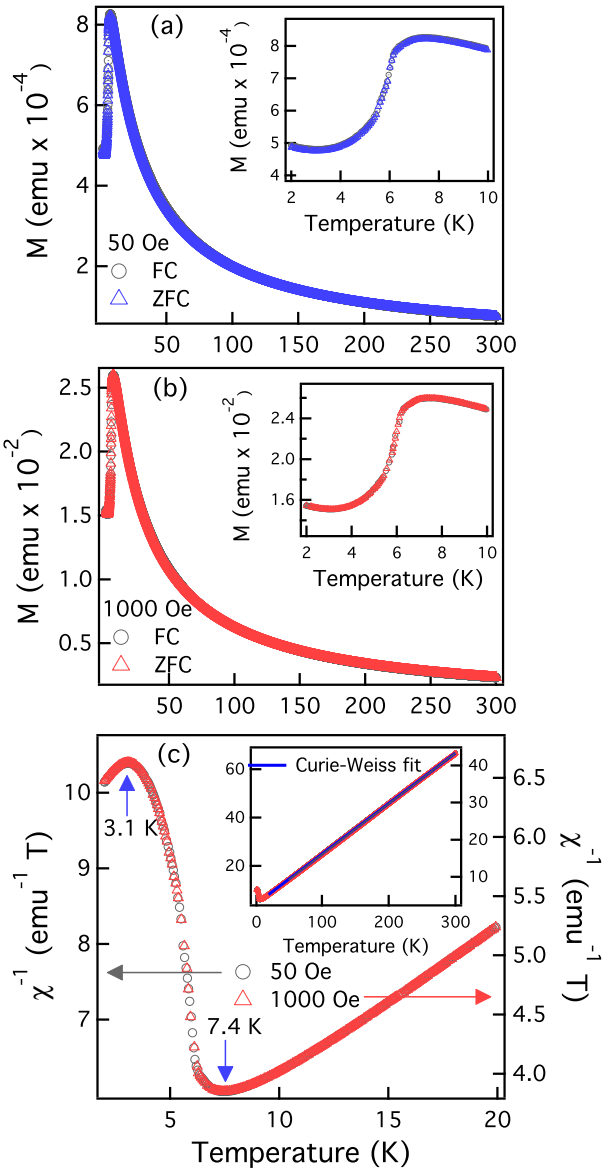

FIG. 6. (Color online) Temperature-dependent of dc magnetization from FC and ZFC with an applied magnetic field of (a) 50 Oe and (b) 1000 Oe (Inset: the magnified image of magnetization in temperature range 2-10K). (c) The inverse magnetic susceptibility, which clearly shows the two transitions at 7.4 K and 3.1 K. The inset shows the Curie-Weiss fit for the temperature range 20-300 K.

7.4 K.

E. DISCUSSION

Our results from ZF-muSR, where the relaxation rate, a broad peak with up and down pattern agrees with already observed magnetic transitions at T_{mag1}, T_{mag2}, and T_{mag3}. The temperature-dependent asymmetry curve from the fit, the inset of 1 (a) shows that the asymmetry starts to drop around at 7.5K,

TABLE I. Expected values of the μSR critical exponents β, w and γ for different magnetic models[23]. The critical exponents of $TbTe_3$ we have, compared to different models are given in the last row of the table.

model	β	w	γ
Mean field	1/2	0	1
Ising 2D	1/8	3/2	7/4
Ising 3D	0.326	0.717(FM)	1.36
		0.596(AFM)	
XY 3D	0.346	0.309	1.318
Heisenberg 3D	0.369	1.026(FM)	1.396
		0.328(AFM)	
$TbTe_3$	(TBC)	0.81(5), $T<T_N$	1.0(1)
		0.63(5), $T>T_N$	

suggesting the the forming of LRMO. The gray area denotes the region where the the significant 2D magnetic correlation is likely in play.[16] dramatic drop of asymmetry in the range 7.5-5.8 K (the gray area), approves the existence of 2D like magnetic correlation[16]. Furthermore Pfuner *et al*., suggested that the long-range antiferromagnetic order in $TbTe_3$ is set up below $T_{mag1}\sim5.8$ K with the incommensurate modulations, which is locked-in to the commensurate magnetic structure below $T_{mag3}\sim5.3$ K.[16]

The results of temperature-dependent LF-μSR measurements at 50 G confirm the antiferromagnetic phase transition at T_N=6.3 K (see Fig.3 (b)), which is close to T_{mag1}. The critical exponents obtained from LF data of $TbTe_3$ above and below T_N are w=0.63(5) and w=0.81(5), respectively. The critical exponents from theoretical models are listed in table I. When we compare our critical exponent values with the values in the table, w = 0.63(5) approaching T_N from above suggests the transition at 6.3 K to be Ising 3D antiferromagnetic (AFM). This agrees with the type of magnetic transition at T_{mag1} from the neutron results[16], although one would expect 2D-like behaviour to occur in this compound. However, w = 0.81(5) from $T < T_N$ is more close to ferromagnetic (FM) configuration, reflecting the underlying FM phase that appears in the multiphase transitions below 6 K. The obtained exponent γ = 1.0(1) from TF-μSR data is below the theoretical value of 1.36 for the Ising 3D model, which is likely a result of the quasi-2D properties of the material.

The three exponents are related to the dynamic exponent z by $z = d(2\beta + w)/(2\beta + \gamma)$. If we assume the transition as Ising 3D, and take β = 0.326, we will get $z = 0.56(4)d = 1.7(1)$, which agrees with the theoretical predictions[27,28] when one takes $d = 3$. In addition, the critical exponents are different on the two sides of the transition as theoretically discussed[29], due to the multiple transitions within the small temperature range. Nevertheless, it is vital to extract β in future from direct measurements of the order parameter below T_N.

When we look at the magnetometry data, the first transition at 7.4 K is the AFM transition as suggested earlier by the critical analysis, it is likely that the domains forms slightly earlier than the $T_N\sim6.3$ K probed by muons.There is probably a region with significant 2D correlation taking in part.[16] The

second transition at 3.1 K may suggest FM features, the transition temperatures are slightly differs from the μSR results, probably due to the different temperature responses between the bulk magnetometry and the local probe.

The effective moment of Tb^{3+} equals μ_{eff} = 5.9933(3) μ_B and 7.6564(3) μ_B from the 50 Oe and 1000 Oe results, respectively. The values are lower than the theoretical value of 9.72 μ_B for the ground state with J = 6[30]. They are also smaller than the value of 9.67(1) in the recent reported 2D spin liquid $TbInO_3$[31], where the anisotropy ratio between the in-plane and perpendicular direction χ_{ab}/χ_c is between 3∼5. The significantly reduced moment in the present $TbTe_3$ is likely due to the large anisotropies in this 2D CDW compound.

Furthermore, the coexistence of CDW and magnetic order in different materials has been studied by different experimental techniques[32–35], providing valuable information about magnetism and charge ordering, but the interplay between magnetism and CDW remains unclear. For example, in $RENiC_2$, the presence of magnetic field suppresses the CDW by Zeeman splitting of electronic bands[33]. However, the reverse situation in another kind of material has been observed[35], where the higher magnetic field improves the nesting condition for the formation of CDW phase. The CDW could also result in even weaker magnetic interaction by reducing the conduction electron density of states[34]. In $Yb_5Ir_4Si_10$, the magnetic order does not affect the CDW order directly, with no evidence of coupling detected between them [32]. Nevertheless, the coexistence of magnetic order and CDW remains unclear and further investigations are certainly needed.

IV. CONCLUSION

We have studied the complex magnetic phase transitions and the critical phenomena in the 2D CDW material $TbTe_3$. ZF-μSR has evidenced the multiple transitions, with a dramatic asymmetry loss from 7.5 K to the LRMO states. We observed a broad peak around the three transitions, with some scatter on the points that agrees quite well with the transition temperatures obtained from other techniques. A magnetic field of 50 G was applied to decouple the electronic spin from the nuclear moment. The temperature dependent LF-μSR measurements show a clear transition at T_N = 6.3 K. The scaling analysis gives the critical exponent w of 0.63(5) above and of 0.81(5) below T_N. It suggests the Ising 3D typed AFM transition when cooling down to 6.3 K, but likely FM phases appearing at lower temperatures. The critical exponent γ = 1.0(1) obtained from TF frequency shift analysis is close to Ising 3D model but smaller than the theoretical value, probably due to the 2D features in this compound. The AFM nature of the first sharp transition was also supported by the dc magnetization measurements, although with a slightly higher transition temperature at 7.4 K. However, there is indeed a second transition occurring at 3.1 K, which corresponds to the FM feature as observed by μSR. The Curie-Weiss analysis gives negative θ of around -18 K, but with a much reduced effective moment of about 6 μ_B, which is likely due to the significant anisotropic features of this 2D CDW material. Indeed the multiple magnetic phase transitions observed both by μSR and magnetometry measurements, present unique criticality regarding the spin fluctuations and magnetic order. Our study has presented a new method of exploring the multiple magnetic transitions in $TbTe_3$, and of studying the critical phenomena associated with the transitions, taking advantages of using muons as a local probe. The fast time resolution to extract the critical exponent β from ZF precessions will be useful to explain the criticality, thus we have proposed for beamtime at the SμS facility of the Paul Scherrer Institut. For studying the exchange couplings and single-ion anisotropy, more appropriate techniques such as inelastic neutron scattering would be needed and to investigate the interlink between magnetism and CDW in $TbTe_3$, the structure refinement below 10 K will be required.

Acknowledgment

We acknowledge ISIS facility for providing the muon beamtime, and are grateful for the help from RAL staff both for the muon and magnetization measurements. We gratefully acknowledge Kerstin Kuespert and Alfred Suttner for growth of single crystals of $TbTe_3$ at the Laboratory of Crystallography in University of Bayreuth. For financial support KR acknowledges HEC Pakistan(PPCR grant), AJD acknowledges EPSRC, ZY acknowledges the funding for the PhD studentship from China Scholarship Council, SvS and NvW acknowledges Deutsche Forschungsgemeinschaft (DFG, German Research Foundation-265092781) and a fellowship of the University of Bayreuth (A 4576-1/3).

* Corresponding author: kaneez.rabia@comsats.edu.pk

1 G. Grüner, *Density Waves in Solids*, Advanced book program: Addison-Wesley (Perseus Books Group, 2000).

2 N. Ru, J.-H. Chu, and I. R. Fisher, Phys. Rev. B **78**, 012410 (2008).

3 A. Banerjee, Y. Feng, D. M. Silevitch, J. Wang, J. C. Lang, H.-H. Kuo, I. R. Fisher, and T. F. Rosenbaum, Phys. Rev. B **87**, 155131 (2013).

4 Y. Iyeiri, T. Okumura, C. Michioka, and K.Suzuki, Phys. Rev. B **67**, 144417 (2003).

5 H. Chudo, C. Michioka, Y. Itoh, and K. Yoshimura, Phys.Rev. B **75**, 045113 (2007).

6 N. Ru and I. R. Fisher, Phys. Rev. B **73**, 033101 (2006).

7 B. F. Hu, B. Cheng, R. H. Yuan, T. Dong, and N. L. Wang, Phys. Rev. B **90**, 085105 (2014).

8 B. F. Hu, P. Zheng, R. H. Yuan, T. Dong, B. Cheng, Z. G. Chen, and N. L. Wang, Phys. Rev. B **83**, 155113 (2011).

9 F. Pfuner, L. Degiorgi, J.-H. Chu, N. Rub, K. Shin, and I. Fisher, Physica B **404**, 533 (2009).

10 M. Lavagnini, A. Sacchetti, C. Marini, M. Valentini, R. Sopracase, A. Perucchi, P. Postorino, S. Lupi, J.-H. Chu, I. R. Fisher, and L. Degiorg, Phys. Rev. B **79**, 075117 (2009).

[11] A. Sacchetti, L. Degiorgi, T. Giamarchi, N. Ru, and I. R. Fisher, Phys. Rev. B **74**, 125115 (2006).
[12] A. Sacchetti, E. Arcangeletti, A. Perucchi, L. Baldassarre, P. Postorino, S. Lupi, N. R. andI. R. Fisher, , and L. Degiorgi, Phys. Rev. Lett. **98**, 026401 (2007).
[13] M. Saint-Paul, C. Guttin, P. Lejay, O. Leynaud, and P. Monceau, Solid State Commun. **240**, 1519 (2016).
[14] P. Monceau, Physica B: Condensed Matter **460**, 2 (2015).
[15] K. Deguchi, T. Okada, G. F. Chen, S. Ban, N. Aso, and N. K. Sato, Journal of Physics: Conference Series **150**, 042023 (2009).
[16] F. Pfuner, S. N. Gvasaliya, O. Zaharko, L.Keller, J. Mesot, V. Pomjakushin, J.-H. Chu, I. R. Fisher, and L.Degiorgi, J. Phys.: Condens. Matter. **24**, 036001 (2012).
[17] N. Ru, C. L. Condron, G. Y. Margulis, K. Y. Shin, J. Laverock, S. B. Dugdale, M. F. Toney, and I. R. Fisher, Phys. Rev. B **77**, 035114 (2008).
[18] P. Dalmas de Reotier and a. Yaouanc, J. Phys.: Condens. Matter **9**, 9113 (1997), arXiv:9710235 [cond-mat].
[19] A. Yaouanc and P. Dalmas de Réotier, *Int. Ser. Monogr. Phys.* (Oxford University Press, 2011) pp. 1–486.
[20] L. Nuccio, L. Schulz, and A. J. Drew, Journal of Physics D: Applied Physics **47**, 473001 (2014).
[21] A. J. Drew, F. L. Pratt, T. L. S. J. Blundell, P. J. Baker, R. H. Liu, G. Wu, X. H. Chen, I. Watanabe, V. K. Malik, A. Dubroka, K. W. Kim, M. Rössle, and C. Bernhard, Phys. Rev. Lett. **101**, 1 (2008), arXiv:arXiv:0805.1042v2.
[22] F. L. Pratt, P. J. Baker, S. J. Blundell, T. Lancaster, M. A. Green, and M. Kurmoo, Phys. Rev. Lett. **99**, 1 (2007).
[23] F. Pratt, T. Lancaster, P. Baker, S. Blundell, W. Kaneko, M. Ohba, S. Kitagawa, S. Ohira-Kawamura, and S. Takagi, Physica B **404**, 585 (2009).
[24] T. Wasiutyński, M. Bałanda, M. Czapla, R. Pełka, P. M. Zieliński, F. L. Pratt, T. Korzeniak, R. Podgajny, D. Pinkowicz, and B. Sieklucka, Journal of Physics: Conference Series **303**, 012034 (2011).
[25] N. Ru, *Charge density wave formation in rare-earth tritellurides*, Ph.D. thesis, Stanford University (Stanford, CA, USA, 2008) (2008).
[26] J. S. Blundell, Contemp. Phys **40**, 175 (1999).
[27] G. F. Mazenko and O. T. Valls, Phys. Rev. B **24**, 1419 (1981).
[28] S. Wansleben and D. P. Landau, J. Appl. Phys **61**, 3968 (1987).
[29] F. Léonard and B. Delamotte, Phys. Rev. Lett. **115**, 200601 (2015).
[30] Carlin and R. L., *Magnetochemistry* (Springer Berlin Heidelberg, Berlin, Heidelberg, 1986).
[31] L. Clark, G. Sala, D. D. Maharaj, M. B. Stone, K. S. Knight, M. T. F. Telling, X. Wang, X. Xu, J. Kim, Y. Li, S.-W. Cheong, and B. D. Gaulin, Nat. Phys **15**, 262 (2019).
[32] Z. Hossain, M. Schmidt, W. Schnelle, H. S. Jeevan, C. Geibel, S. Ramakrishnan, J. A. Mydosh, and Y. Grin, Phys. Rev. B **71**, 060406 (2005).
[33] K. K. Kolincio, M. Roman, M. J. Winiarski, J. Strychalska-Nowak, and T. Klimczuk, Phys. Rev. B **95**, 235156 (2017).
[34] F. Galli, R. Feyerherm, R. W. A. Hendrikx, E.Dudzik, G. J. Nieuwenhuys, S. Ramakrishnan, S. D. Brown, S. van Smaalen, and J. A. Mydosh, J. Phys.: Condens. Matter **14**, 5067 (2002).
[35] J. Brooks, D. Graf, R. Henriques, E. Choi, M. Almeida, J. Dias, and M. Matos, CURR. APPL. PHYS **6**, 913 (2006).